A Resistor-Based Temperature Sensor for MEMS Frequency References

Mina Shahmohammadi, Kianoush Souri, and Kofi A.A. Makinwa
Electronic Instrumentation Laboratory, Delft University of Technology, Delft, the Netherlands

***Abstract*— This paper presents a CMOS temperature sensor intended for the temperature compensation of MEMS frequency references. It is based on a Wien bridge RC filter, whose phase-shift, due to the temperature dependency of the resistors used, is temperature dependent. This phase shift is then digitized by a phase domain sigma-delta modulator. The sensor was implemented in 0.18µm CMOS, consumes 36 µW and achieves 6mK resolution in a conversion time of 100msec. After batch calibration and a 3-point trim, it achieves ±0.15°C (3σ) inaccuracy over the industrial range (-40°C to 85°C).**

I. Introduction

In recent years, frequency references based on MEMS resonators have demonstrated performance that is comparable with that of traditional quartz-crystal references [1, 2]. However, compensating for the relatively large temperature coefficient of MEMS resonators (about -30ppm/°C) still poses a major challenge, which is usually met with the help of a co-integrated temperature sensor. The accuracy and jitter of the frequency reference is then limited by the sensor's accuracy and resolution. For example, achieving sub-ps jitter requires sub-mK resolution in a 5 Hz bandwidth [2].

Achieving sub-mK resolution is a difficult challenge, and one that has not yet been met by traditional BJT-based temperature sensors [3]. In this regard, resistor-based temperature sensors seem to be much better candidates [1-2]. In [1], a temperature-dependent current derived from an n-well resistor, is used to drive a ring oscillator. This results in a temperature-dependent output frequency with an equivalent resolution of 40 mK in a 7.5 msec conversion time, while consuming 30 µW. After a 3-point trim, the frequency reference's inaccuracy is less than ±10 ppm, which corresponds to a temperature sensing inaccuracy of about ±0.33°C. In [2], a temperature-dependent resistor and an adjustable reference resistor are incorporated in a bridge. The reference resistor is realized by a switched capacitor network whose resistance is a function of its clock frequency. A feedback loop keeps the bridge balanced by adjusting this frequency via a fractional-N divider driven from a reference clock. The resulting division factor is then a measure of temperature. This sensor achieved state of the art resolution of 100 µK in a 100 msec conversion time, while consuming 13mW [6]. After a 6-point trim, the complete frequency reference achieves an inaccuracy of ±0.5 ppm, which corresponds to a temperature sensing inaccuracy of about ±0.015°C.

Although resistor-based temperature sensors can achieve high resolution, their accuracy is limited by the spread and nonlinear temperature dependence of integrated resistors. As a result, they require multi-point trimming. However, this makes them a good match for MEMS or quartz-crystal resonators, whose own non-linear temperature dependence means that they also require multi-point trimming [1].

In this work we will discuss the design of a resistor-based temperature sensor with an inaccuracy of ±0.15°C from -40°C to 85°C after 3-point trimming. In the next section, the system design of this sensor will be discussed. Section III is devoted to the circuit implementation, and is followed by a discussion of the measurement results in section IV. The paper ends with conclusions.

II. System Design

Measuring temperature requires two signals: a temperature dependent signal and a reference signal. While most of the resistors available in standard CMOS technology exhibit significant temperature coefficients (1000s of ppm/°C), no well-defined reference resistors exist. In a MEMS frequency reference, however, a well-defined frequency is available. This can be used as a reference signal, provided that a temperature-dependent signal time domain is also available.

One way of generating such a signal is by exploiting the fact that the phase-shift of an RC filter depends on its input frequency and on the value of its resistors and capacitors. Since MIM capacitors are quite stable over temperature while resistors are relatively temperature dependent, an RC filter driven by a reference frequency will exhibit a temperature-dependent phase-shift.

To minimize its size and complexity, a 1st or 2nd order RC filter should be used. Of these, low-pass and band-pass filters are desirable since they inherently impose a bandwidth limit on the resistors' thermal noise. Figure. 1 shows two possible candidates: a 1st order low-pass and a Wien bridge band-pass filter. Their transfer functions and phase-shifts are given by:

Low pass:
$$H(j\omega) = \frac{1}{1 + RCj\omega} \tag{1}$$

$$\phi_{RC-LP}(j\omega) = -\tan^{-1} RC\omega \tag{2}$$

978-1-4799-0645-1/13/$31.00 ©2013 IEEE

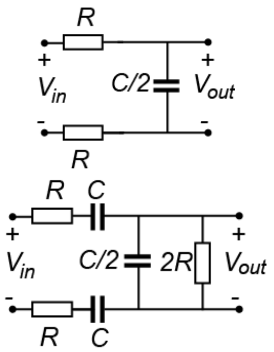

Figure 1. 1st order low pass filter(top) and Wien bridge filters (bottom)

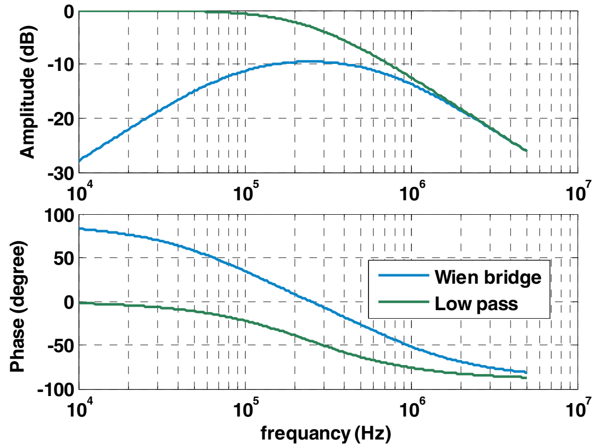

Figure 2. Bode plots of the low pass and Wien bridge filters.

$$\text{Wien bridge:} \quad H(j\omega) = \frac{RCj\omega}{(1 - R^2C^2\omega^2) + 3RCj\omega} \qquad (3)$$

$$\phi_{RC-WB} = -\tan^{-1}\frac{(R^2C^2\omega^2 - 1)}{3RC\omega} \qquad (4)$$

The corresponding Bode plots are shown in Fig. 2. The frequency $\omega = 1/RC$ is the low-pass filter's cut-off frequency and the Wien bridge's center frequency, respectively. At this frequency, the phase-shift ϕ_{RC} is $\pi/4$ and 0 for the low-pass and Wien bridge filters, respectively. Figure 3 shows how these phase shifts vary over the industrial temperature range (-40°C to 85°C) for $R = R_0\left(1 + \alpha(T - T_0)\right)$, with α =0.15% and f_0= 250 kHz. After a 2nd order polynomial fit (3-point trim), the non-linearity of these plots is shown in Fig. 4. It can be seen that the non-linearity of the low-pass filter exceeds the 0.1°C target. For this reason, we chose the Wien bridge filter over the more area-efficient low-pass filter.

From Fig. 3, it can be seen that over the industrial range, the total phase-shift of the Wien bridge is quite small, only about 8°, and so a precision phase read-out circuit is needed. A phase-domain sigma-delta modulator (PDΣΔM) is well-suited for this purpose [4,5]. This is quite similar to a conventional amplitude-domain ΣΔM, except that the input and reference signals are in the phase domain. As shown in Fig. 5, the filter is driven by a square wave f_{drive}, while the references consist of two digitally phase-shifted square-waves $f_{drive}(\phi_0)$ and $f_{drive}(\phi_1)$.

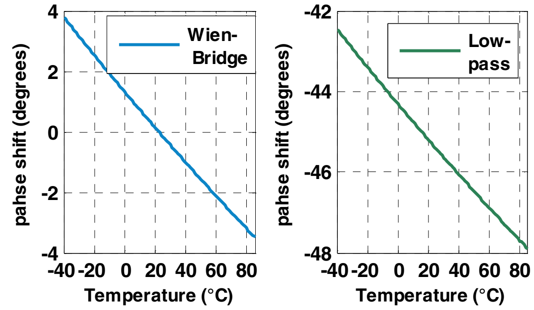

Figure 3. Wien bridge and low-pass phase shift over the industrial range.

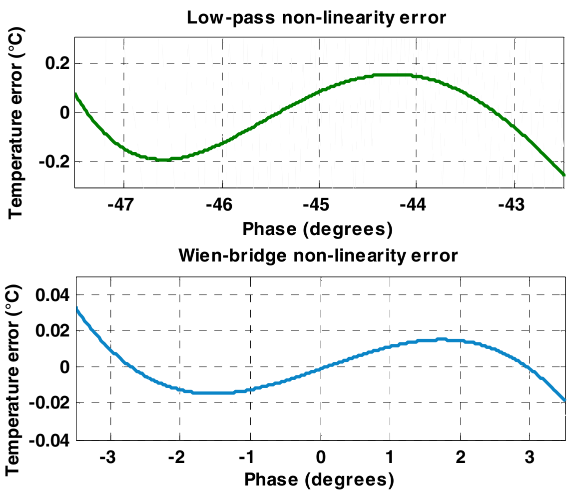

Figure 4. Phase shift nonlinearity.

The modulator consists of a multiplying phase detector (a chopper), an integrator, a quantizer and a single-bit DAC Depending on the modulator's bit stream, *bs*, the output of the filter is multiplied by one of the two phase references, creating a phase error signal that is then integrated. At steady-state, the dc input to the integrator has an average value of zero, and so the bit stream average μ, will be equal to a weighted sum of the two phase references, and be a digital representation of φ_{RC}.

Since the integrator's dc input has a zero average, then:

$$\mu\frac{1}{2}A_1\cos(\phi_1 - \phi_{RC}) + (1-\mu)\frac{1}{2}A_1\cos(\phi_0 - \phi_{RC}) = 0 \qquad (5)$$

This can be rewritten as:

$$\mu = \frac{\cos(\phi_0 - \phi_{RC})}{\cos(\phi_0 - \phi_{RC}) - \cos(\phi_1 - \phi_{RC})}. \qquad (6)$$

Due to the cosine characteristic of the phase detector, this is a somewhat non-linear function of ϕ_{RC}. For maximum linearity, the phase-references should straddle a range that is ~90° degrees out of phase with ϕ_{RC} and is just wide enough to handle its expected variation over temperature (8°) and process (±30%). In this work, phase references ϕ_0=67.5° and ϕ_1=112.5° were used. This results in an additional non-linearity of only 0.02°C after a 2nd order fit.

The temperature-sensing resolution of a Wien bridge filter can be determined by noting that at its center frequency ω_0, the real part of its output impedance is given by:

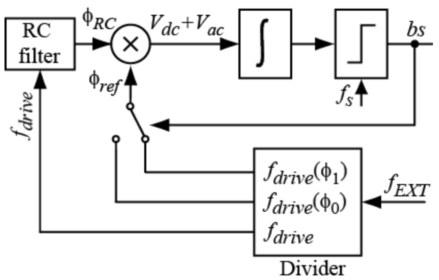

Figure 5. Phase domain sigma-delta modulator.

$$Z_{\mathrm{Re}}(\omega_0) = \frac{2R}{3} \tag{7}$$

So the noise spectral density of the filter's output will be:

$$v_n = sqrt(8kTR/3). \tag{8}$$

We also need to know the sensitivity S_{WB} of the chopper's dc output, V_{dc}, to temperature. Using (4), this can be expressed as:

$$S_{WB} = \frac{dV_{dc}}{dT} = \frac{dV_{dc}}{d\phi_{RC}} \cdot \frac{d\phi_{RC}}{dT} \tag{9}$$

Where,

$$\frac{d\phi_{RC}}{dT} = \frac{d\phi_{RC}}{dR} \cdot \frac{dR}{dT} = \frac{2}{3R_0} \cdot \alpha R_0 = \frac{2\alpha}{3} \tag{10}$$

Since the Wien bridge is a band-pass filter, and the phase detector is a chopper, we can obtain a good approximation of S_{WB} by just considering the first harmonics of the drive signal. For a square wave of amplitude A, the filter's output is,

$$V_{filter} = \frac{4}{\pi} \cdot \frac{A}{3} \sin(\omega_0 + \phi_{RC}) \tag{11}$$

This signal will be chopped by another square wave with the same frequency,

$$V_{ref} = \frac{4}{\pi}[\sin(\omega_0 + \phi_{ref}) + \frac{1}{3}\sin(3\omega_0 + \phi_{ref}) + \cdots] \tag{12}$$

The resulting dc component is only due to the first harmonic and is given by:

$$V_{dc} = \frac{16}{\pi^2} \cdot \frac{A}{6} \cos(\phi_{RC} - \phi_{ref}) \tag{13}$$

At room temperature, where $\sin(\phi_{ref}) = \sin(\phi_0) = \sin(\phi_1)$ the sensitivity of the chopper's dc output to phase is given by:

$$S_{WB} = \frac{16}{\pi^2} \cdot \frac{A}{6} \sin(\phi_{ref}) \times \frac{2\alpha}{3}. \tag{14}$$

Assuming t_{conv}=100 msec, ϕ_{ref}=67.5 degrees, R_0=135 kΩ, α=0.15% and A=1.8 V; then from (8)-(11), dT=*192.1* μK. This result shows that the combination of a reference frequency, a Wien bridge filter and a chopper phase detector can achieve sub-mK resolution.

III. CIRCUIT DESIGN

As shown in Fig. 5, the PDSDM requires an integrator. To minimize its power dissipation, this was implemented as a passive rather than an active integrator. However, the filter is driven by a rail-to-rail square-wave (1.8V) and so its output amplitude is too large for linear handling by a traditional Gm-C integrator. Instead, the circuit of Fig. 6 is used. Here the output resistors of the WB are connected to the virtual ground of a current buffer, which then conveys the phase-shifted current to an integrating capacitor via a chopper demodulator. This approach also eliminates the mismatch and 1/*f* noise of the current sources $M_{1,2}$. The inclusion of a chopper in the buffer's p-side does the same for the current sources $M_{7,8}$. A gain booster is used to ensure that the current buffer's input impedance is much lower than the filter's output impedance. The single-bit DAC is a comparator, which is realized by three pre-amplifiers followed by a static latch.

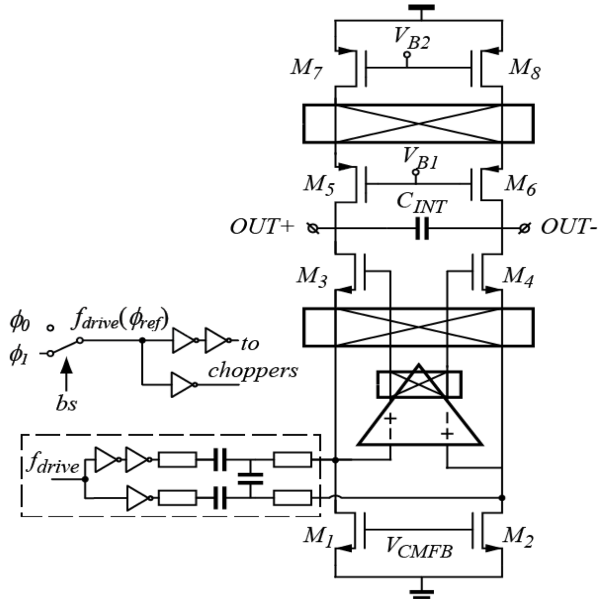

Figure 6. Current buffer circuit.

In order to investigate the properties of different kinds of resistors, four filters were built from identical MIM capacitors and four different types of resistors: N+ diffusion, P+ diffusion, N-poly and N-well. The temperature coefficients of these resistors and the corresponding phase shift over the industrial range can be found in Table I.

The drive frequency f_{drive} = 250 kHz was chosen to be higher than the 1/*f* corner frequency of the current sources. The choice of R=135 kΩ then results in C=4.7 pF, which is large enough to swamp the resistors' parasitic capacitances. As discussed earlier, the modulator uses reference phases φ_0=67.5 and φ_1=112.5 degrees. These references, together with f_{drive} are generated digitally from a 4 MHz master clock. Finally the integration capacitor, C_{INT}, is 40 pF and the modulator's sampling frequency f_s, is 125 kHz.

IV. MEASUREMENT RESULTS

To verify the proposed readout scheme, a chip was fabricated in a 0.18 μm TSMC process. It has an active area of 0.35mm^2 and was packaged in a 16-pin ceramic DIL package. Figure 7 shows the chip photomicrograph. The chip draws 36μW from a 1.8 V supply. In a 100 ms conversion time, the standard deviation of the decimated bit stream corresponds to a temperature resolution of 3 mK for the N-well resistor and about 6mK for the other resistor types. This

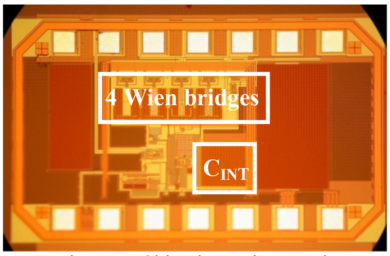

Figure 7. Chip photomicrograph

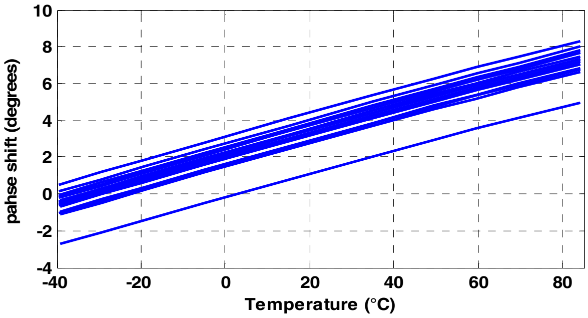

Figure 8. N-poly filter phase shift (16 chips).

result is worse than that predicted in section II and was found to be mainly due to the noise of the current buffer.

To measure the sensor's inaccuracy, 18 chips from one batch were characterized over the industrial range. The phase-shift generated by the N-poly filter is shown in Figure 8. After a 2nd order polynomial fit, using three data points, the resulting 3σ spread was about ±0.15°C, but was dominated by a much larger systematic error. For a given batch, however, this error can be removed by a *fixed* 3rd-order polynomial, (Fig. 9). A similar approach was used to process the characteristics of the other filters and the results are summarized in Table I. The N-poly resistor is the most accurate, while the N-well filter has about 2x more resolution, but at the expense of significantly more non-linearity, which required a fixed 4th order polynomial. Table II summarizes the performance of the N-poly filter and compares it with that of other resistor-based sensors.

Table I Performance of the different resistor types

Resistor Type	Temperature coefficient	Inaccuracy (after 2nd order fit)	Order of correction polynomial	Total phase Shift
N+ diffusion	0.15%	±0.15°C	2	8 degrees
P+ diffusion	0.15%	±0.25°C	3	7.8 degrees
N-poly	-0.15%	±0.15°C	3	7.5 degrees
N-Well	0.3%	±0.25°C	4	15 degrees

V. CONCLUSION

A resistor-based temperature sensor has been implemented in a 0.18µm TSMC process. The temperature-dependent phase shift of a Wien bridge RC filter is digitized by a phase-domain sigma delta modulator. It achieves 3mK - 6mK resolution in a 100ms conversion time. After a 2nd order polynomial fit, and the removal of systematic non-linearity, the proposed sensor achieves ±0.15°C inaccuracy over the industrial temperature range: -40°C to 85°C.

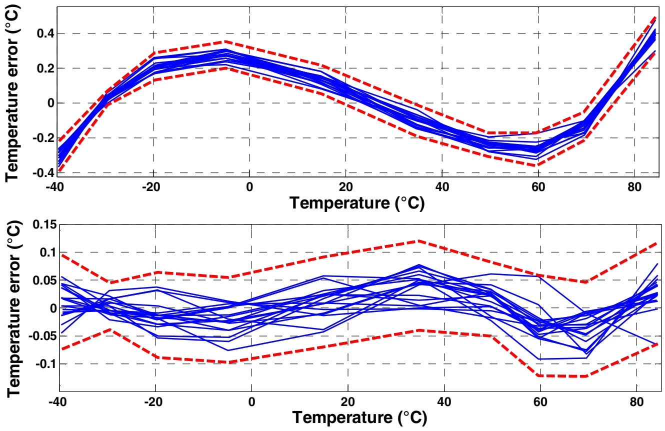

Figure 9. Inaccuracy after a 2nd order polynomial fit (top) and after removing systematic error with a third order polynomial (bottom) for N-poly filter.

Table II Performance summary and comparison to previous work

Parameter	This Work	[1]	[2]
Technology	0.18µm	0.18µm	0.18µm
Chip area	0.35mm²	0.044 mm²	0.18 mm²
Power consumption	36µW	30 µW	13mW
Temperature range	-40°C - 85°C	0°C - 100°C	-40°C - 85°C
Inaccuracy (trim points)	±0.15°C † (3)	±0.33°C †† (3)	±0.015†† (6)
Resolution (T_{conv})	0.006°C (100msec)	0.04°C (7.5msec)	100µ°C (100msec)
FOM(nJK²)	0.13	0.36	0.013

†: 3σ, ††:Min/Max

ACKNOWLEDGMENT

The work presented has been performed within the project Go4Time (www.go4time.eu), which is funded by the EC FP7 research program.

REFERENCES

[1] D. Ruffieux *et al.*, "Silicaon resonator based 3.2µW real time clock with ±10 ppm frequency accuracy," *J. Solid-State Circuits*, vol. 45, is. 1, pp. 224 – 234, Jan. 2010.

[2] M. H. Perrott *et al.*, "A temperature-to-digital converter for a MEMS-based programmable oscillator with <±0.5 ppm frequency Stability and <1-ps Integrated Jitter", *J. Solid-State Circuits*, vol. 48, is. 1, pp. 276 – 291, Jan. 2013.

[3] K. Souri, et *al.*, "A CMOS Temperature Sensor With a Voltage-Calibrated Inaccuracy of ±0.15°C (3) From -55°C to 125°C," *J. Solid-State Circuits*, vol. 48, is. 1, pp. 292 – 301, Jan. 2013.

[4] S. M. Kashmiri *et al.*, "A Temperature-to-Digital Converter Based on an Optimized Electrothermal Filter," *J. Solid-State Circuits*, vol. 44, is. 7, pp. 2026 – 2035, July. 2009.

[5] C.P.L. van Vroonhoven and K.A.A. Makinwa, "A CMOS Temperature-to-Digital Converter with an inaccuracy of ±0.5°C (3σ) from -55 to 125°C," *IEEE ISSCC* Dig. Tech. Papers, pp. 576–577, February 2008

[6] K.A.A. Makinwa, "Smart Temperature Sensor Survey", [Online]. Available: http://ei.ewi.tudelft.nl/docs/ TSensor _survey.xls.